 DOI: 10.1002/masy.200950932

Polymer Chain Collapse in Supercritical Fluids. 2. Experimental Evidence

C. H. Ortiz-Estrada,[1] *G. Luna-Bárcenas,*[*2] *J. F. J. Alvarado,*[3] *G. González-Alatorre,*[3] *I. C. Sanchez,*[4] *N. Flores Ramírez,*[5] *Salomón R. Vásquez García,*[6] *J. Castillo-Tejas,*[7] *O. Manero-Brito*[8]

Summary: The phase behavior of a polymer in a supercritical solvent at the LCST equilibrium limits is described in this work, in the proximity of θ point, proposing the use of a conformational parameter, Ψ. The results obtained by molecular simulation in an NVT ensemble have been correlated by extensive, varied experimental information. The relationship between polymer/solvent solubility parameters has shown that the behavior of these systems is a function of the energetic structure-interaction relationship between the polymer chain and the solvent. Ψ results in a generalized parameter indicative of the phase stability of the solution. At greater magnitudes, the solution becomes unstable, requiring elevated pressure to stabilize. However, stable solutions are found at lower pressures when Ψ approaches 1. The experimental evidence, together with the determination of the solubility parameter with the Sanchez-Lacombe equation (also obtained from the literature) strengthens this observation. The analysis of the polar contribution on the Hansen Parameter (HSP) enables their effect to be studied in systems where high polar interactions between the polymer and solvent (as in the case of biopolymers) are expected.

Keywords: molecular simulation; phase behavior; polymer chain collapse

Introduction

In recent decades, the use of supercritical fluids as processing agents in the polymer and biopolymer industries has aroused interest. Their unique physical chemical properties have brought about their use in separation processes such as fractionation and purification of monomers and polymers in polymeric solutions,[1–2] latex stabilization,[3] impregnation and coloring,[4] extraction and depositing particles.[5–6] Some homo-polymers and co-polymers have been synthesized in supercritical CO_2 via homogenous polymerizations, precipitations, dispersion, emulsion and suspension.[7–9] Other technological applications include the formation of particles,[10–12] micronization of biopolymers,[13] generation of particles for medical and pharmaceutical applications[14–15] and the formation of nanomaterials.[16]

The dominant phenomenon in all the above applications is represented by the phase separation process owing to changes in the temperature and pressure of the system. In 1960 Freeman and Rowlinson[17] reported that a homogenous solution of polymer can be separated in a phase that is

[1] Departamento de Ingeniería y Ciencias Químicas, Universidad Iberoamericana, México, D. F. 01219 México
[2] Laboratorio de Investigación en Materiales, CINVESTAV Unidad Querétaro, Querétaro, Querétaro 76230 México
E-mail: gluna@qro.cinvestav.mx
[3] Departmento de Ingeniería Química, Instituto Tecnológico de Celaya, Celaya, Guanajuato 38010, México
[4] Chemical Engineering Department, University of Texas at Austin, Austin, TX 78712 USA
[5] Faculty of Wood Engineering and Technology. University Michoacana of San Nicolás de Hidalgo, Morelia, Michoacán 58060, México
[6] Faculty of Chemistry, University Michoacana of San Nicolás de Hidalgo, Morelia, Mich. 58060, México
[7] Chemical Engineering Department, Universidad de Tlaxcala,Tlaxcala, Tlax 90070. Mexico
[8] Instituto de Investigacion en Materiales, UNAM, Mexico, D.F.

rich in polymer and another that is rich in solvent when the temperature of the solution approaches the solvent's critical temperature. That is, the phase behavior (compatibility) of a binary polymer-solvent mixture is characterized either by the lower consolute temperature type (Lower Critical Solution Temperature LCST) or by the upper consolute temperature type (Upper Critical Solution Temperature UCST). This behavior is typical of polymeric systems and is shown schematically in Figure 1. The phase behavior of a polymeric solution in a P-T diagram shows the liquid-liquid separation at low temperature with the presence of the UCST curve, and at a high temperature with the presence of the LCST curve. Note that the LCST curve is found in the region around the critical point of the pure solvent.

The huge difference in physical properties between the polymer and solvent induce physico-chemical interactions in polymeric solutions, showing a complex behavior of phase and stability. In the LCST the separation of phases is due to the difference in thermal expansion between each component. This produces a change in density between the solvent and the polymer, like the effect of ''free volume'' that predominates in the area of the critical point of the solvent. Therefore, the LCST type phase equilibrium is dominated by the highly compressible nature of the solvent

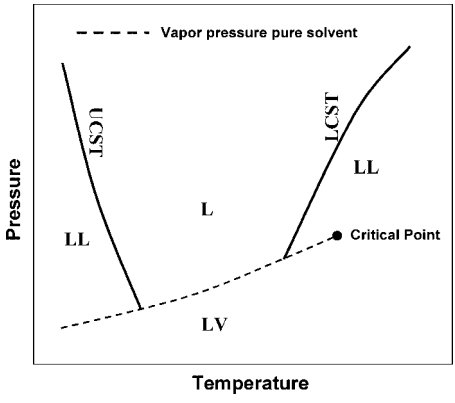

Figure 1.
Diagram pressure-temperature for a mixture polymer-solvent to the near critical point of the pure solvent.

that, in general, tends to form thermodynamically less stable polymeric solutions.

In Part 1, after extensive molecular simulations, it was reported that in a polymeric solution at infinite dilution, the polymer collapses when the solution is heated from the point θ. The θ point is defined as the thermodynamic state in which the second virial coefficient is zero, i.e. when forces of attraction or repulsion are cancelled out. This phenomenon is related to, or moreover represents the LCST type of phase separation (at constant temperature) that is found around the critical point of the pure solvent.

When the temperature is raised above point θ, the chain expands again, indicating that the ''quality'' of the solvent has improved to such an extent that the solution forms a single, homogenous phase. The collapse of the chain represents precisely the existence of an LCST whereas the subsequent expansion is related to the existence of a UCST. This gives way to a closed miscibility loop, depending strongly on the size relationship and energy interaction between the chain segment-solvent that were related by means of the conformational parameter (Ψ) proposed in the part 1. These effects were correlated successfully through Ψ, being observed that this parameter is a measure of the behavior of the polymeric chain in the solution.

It has been reported that the solubility of a polymer in a supercritical CO_2 is related to the surface tension of the pure polymer[18] and this surface tension with the density of the cohesion energy of the polymer. Consequently it can be considered as a measure of the molecular interactions between the polymer-solvent and therefore, between the solubility of the polymer in the solvent.

The Cohesion Energy Density (CED) is directly related to the solubility parameter δ, a property much-used in the estimation of the solubility of various solutes in liquid solvents. The relationship between the solubility parameters of two materials represents the effect of solubility on them.

For example, two materials with similar solubility parameters have sufficient energy to promote their dispersion, and by extension, mixing. However, when the solubility parameters are different, greater energy is required for them to mix, making them incompatible, causing inmiscibility.

The solubility parameter, initially introduced by Hildebrand and Scott[19] is a key property in the selection of solvents in Industry. Their numeric estimation provides a quick and simple technique to predict the solubility of many solutions. Their importance is shown in the diverse applications in the technology and science of polymers (coatings, colorants, paints, plastification, formation of membranes, compatibility studies, etc.).[20–29] Among other recent applications is the extraction of pesticides from the ground by solvents[30] and the physico-chemical properties of fullerenes in organic solvents and polymers.[31]

This property was initially applied for non-associated and non-polar liquids. Nevertheless, the concept was extended to other types of systems such as polymer-solvent and polymer-polymer amongst others. In 1967, Hansen[21] proposed that the concept of the solubility parameter could be extended to polar systems and in the presence of hydrogen bridges. A solubility parameter (HSP) was proposed in relation to the contribution of three intermolecular forces: Dispersion (d), Polarity (p) and Hydrogen Bonds (h).

$$\delta_o^2 = \delta_d^2 + \delta_p^2 + \delta_h^2 \tag{1}$$

The solubility parameter has been the subject of various studies. There is a body of experimental data for a great number and variety of solvents and polymers[21,32–37] along with models for their prediction starting from state equations,[38–41] group contribution methods[42–43] and molecular simulation[44] in the determination of the solubility parameter of polyolefins. In the case of supercritical fluids, the prediction of the solubility parameter as a function of temperature and pressure has also been the subject of study.[45–47]

In this work, the results of the molecular simulation obtained in Part 1 together with the relationship of solubility parameters between the polymer and supercritical solvent are compared. Extensive experimental information of the LCST equilibrium in the region of point θ for various polymer and biopolymer solutions under conditions close to the critical point of the pure solvent are included.

The Effect of Solubilty. A Theoretical Approximation

The solubility of a solute in a solvent has been theoretically associated, via the theory of regular solutions, with the energy of cohesion (CED, cohesive energy density), ξ and with the solubility parameter δ

$$\xi = \frac{\Delta_{vap}u}{v^L} \tag{2}$$

where $\Delta_{vap}u$ the internal vaporization energy and v^L the volume of component i.

$$\delta = \left[\frac{\Delta_{vap}u}{v^L}\right]^{1/2} \tag{3}$$

The relationship between the solubility parameters solvent-solute is a measure of compatibility of the solution that, related to the Flory parameter χ, corresponds to the expression[48]

$$\chi = \frac{v_s}{RT}(\delta_S - \delta_P)^2 \tag{4}$$

where S stands for solvent and P for polymer.

For a good solubility χ should be small, in accordance with the Scatchard-Hildebrand theory for non-polar components. One criterion to define a good solvent for a given polymer is that the solvent-polymer solubility parameters be similar, such that χ approaches zero.

$$\delta_S \approx \delta_P \tag{5}$$

This expression provides a practical guide to the effect a solvent would have on the solubility of a given polymer. The greater the difference in parameters, the more unstable a solution is expected

to be. It would result in an incompatible mixture, and therefore in the inmiscibility of the solution.

The development of state equations of liquid solutions that contain different sized non-polar molecules, in principal, has been based on the lattice theory arising from the Flory-Huggins equation. In this type of system, the components show differences in the behavior of the free volume, and therefore, varying degrees of expansion. This variation should be taken into account for the effect on the properties of the solution and the phase stability.

The lattice theory of a molecular lattice fluid (LF), developed by Sanchez-Lacombe[49–50] from the Flory-Huggins theory, considers empty sites in the lattice, where the fluids can be accommodated in the solution, emulating free volume. The change of volume in the mixture is taken into account, giving a good description of phase behavior.

$$\tilde{\rho}^2 + \tilde{P} + \tilde{T}[\ln(1-\tilde{\rho}) + (1-1/r)\tilde{\rho}] = 0 \quad (6)$$

where r is the number of sites that occupy a segment, $\tilde{T}$, $\tilde{P}$ y $\tilde{\rho}$ are the reduced temperature, pressure and density, respectively defined as:

$$\begin{aligned} \tilde{T} &\equiv T/T^* \\ \tilde{P} &\equiv P/P^* \\ \tilde{\rho} &\equiv \rho/\rho^* \end{aligned} \quad (7)$$

whose characteristic parameters are T^*, P^* and ρ^*, obtained from PVT experimental data and the equilibrium of the pure component.[49]

In their parameters, the LF theory, arising from the Sanchez-Lacombe equation, considers the molecular characteristics of the components via the following relationships,

$$\varepsilon^* = kT^* \quad (8)$$

$$v^* = kT^*/P^* \quad (9)$$

$$r = MP^*/kT^*\rho^* = M/\rho^* v^* \quad (10)$$

In their original pubication,[49] the authors identify ε^* with the interaction energy between nearby segments and v^* with the close packed volume of a segment.

The Sanchez-Lacombe equation therefore takes into account the energetic effect and the size of the segments of the molecule in the behavior of the solution. The total molecular interaction energy $r\varepsilon^*$ is equal to the energy required to convert 1 mol of fluid from the close packed state $\tilde{\rho} \to 1$ to vapor $\tilde{\rho} \to 0$

The identification of $r\varepsilon^*$ with the vaporization energy in the close packed state of the fluid helps towards a simple interpretation of ε^*/v^*. This relationship is defined as the characteristic pressure P^* and is equal to the cohesion energy of the fluid in the close packed state.

$$CED = \Delta_{vap}u/v = r\varepsilon^*/rv^* = P^* \quad (11)$$

At a finite temperature the energy of cohesion is given by[50]

$$CED = P^*\tilde{\rho}^2 \quad (12)$$

and the solubility parameter,

$$\delta = \sqrt{CED} = \tilde{\rho}\sqrt{P^*} \quad (13)$$

In this work, the solubility parameter evaluated by the Sanchez-Lacombe equation will provide an estimate of the behavior of a polymeric solution compared to the results obtained by molecular simulation. This is because the conformational parameter, Ψ defined in Part 1 can easily be related to the solubility parameter, and therefore to the cohesion energy.

Substituting the cohesion energy in relation to the characteristic parameters of the Sanchez-Lacombe equation in the conformational parameter, the expression becomes

$$\Psi = \frac{CED_m}{CED_s} = \frac{\left(P^*\tilde{\rho}^2\right)_m}{\left(P^*\tilde{\rho}^2\right)_s} = \left[\frac{\delta_m}{\delta_s}\right]^2 \quad (14)$$

This relationship will enable the stability of a polymeric solution in a supercritical fluid obtained from experimental results to be compared with those obtained by molecular simulation, providing a clear signal of the solution's behavior.

Strategy

Figure 2 shows the equilibrium limits at T_r vs. P_r conditions of the solvent. The results show that in the supercritical region of the pure solvent, the presence of the LCST are observed that depend on the conformational parameter in relation to the energetic polymer-solvent interaction and the size of the segment-solvent.

The results indicate that when Ψ increases, the chain tends to collapse, provoking instability in the solution and creating a poor solvent, widening the immiscibility region. However, at small magnitudes of Ψ, the solvent becomes efficient (a good solvent). The chain expands and the solution is stable, leading to the region of a phase, reducing the immiscibility region. The further away this parameter is, the greater the pressure required to reach the conditions of solution stability. The figure shows that there is a closed miscibility loop given that the increase in temperature again collapses the chain occurring at the UCST. This phenomenon has not yet been observed experimentally.

These results were compared with varied and extensive experimental information of polymers and biopolymers in different solvents close the supercritical region where the LCST behavior occurs at point θ constructed in the T_r-P_r diagram.

For the comparison of the results obtained from molecular simulation in relation to the conformational parameter Ψ it was necessary to take the experimental data to the same scheme. For that it was necessary to have the solubility parameters of the corresponding polymers and solvents to hand, either obtained from the literature or determined by the Sanchez-Lacombe equation.

As an example consider the equilibrium of the Poly (1H,1H-perfluorooctyl methacrylate) (PFOMA)-CO_2[51] system that displays LCST behavior in the supercritical region of pure CO2. Figure 3 shows the increase in the equilibrium pressure (at the LCST point) with the molecular weight of the PFOMA, observing the point θ at different temperatures as well as its T-P diagram.

In the PFOMA case, the characteristic parameters of the Sanchez-Lacombe (S-L) equation of state were not available. For this reason, it was required to adjust experimental PvT data to the S-L equation. Table 1 reports the adjusted S-L parameters, the solubility parameters for PFOMA and CO_2, and the conformational parameter Ψ.

In Figure 4 the PFOMA T_r -P_r phase diagram is compared to the molecular simulation results. The experimental measurements at different pressures of the

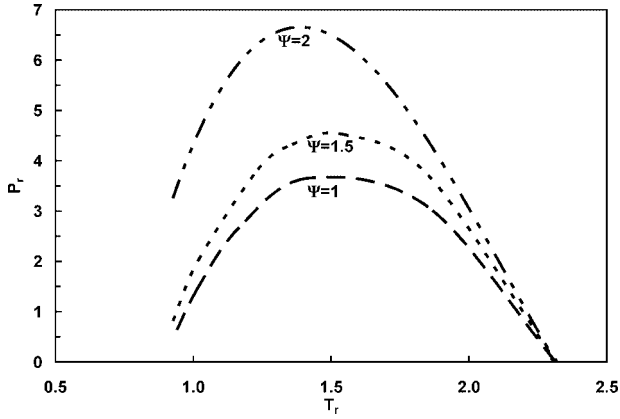

Figure 2.
Equlibrium behavior of a polymer in the supercritical region of the solvent obtained by molecular simulation to different conformational relation between chain segment-solvent.

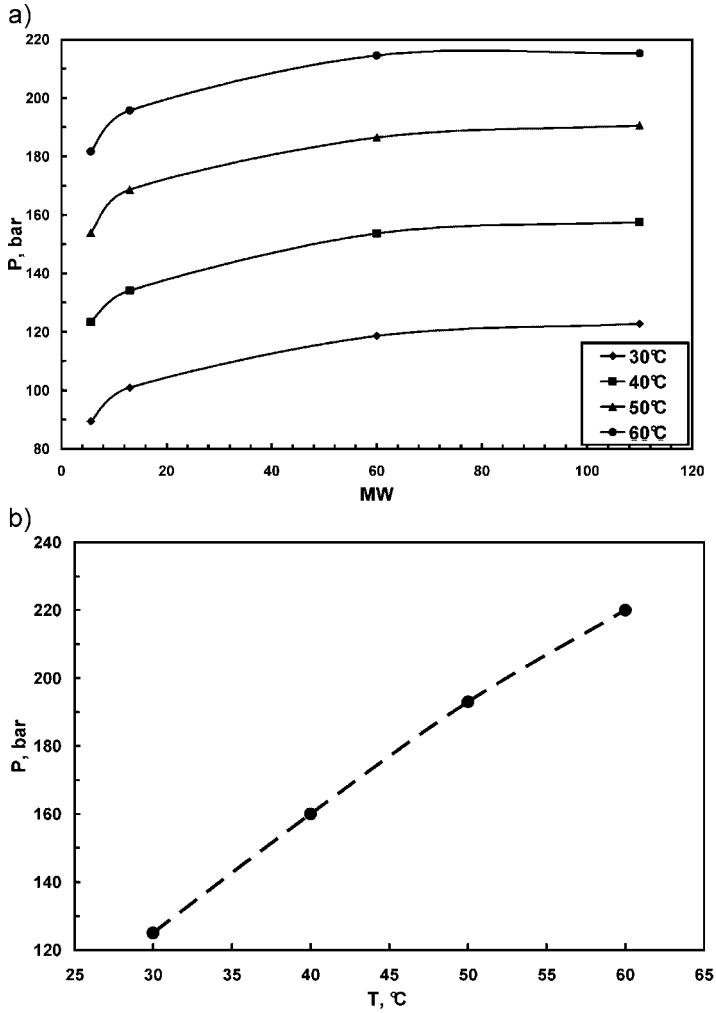

Figure 3.
Critical P-T diagram in relation to the molecular weight of the PFOMA and the θ point.

LCST loci (at the θ point), compared with the molecular simulation, show a great similitude as for the tendency in the behavior of the system. This fact, regarding the proposed conformational parameter, has been corroborated for the first time with experimental information. Even though the conformational parameters Ψ, of the PFOMA-CO_2 solutions were estimated from the S-L parameters along with experimental data, they have shown a favorable stability behavior that was expected for this kind of solutions in agreement with the molecular simulation.

Information

Table 2 shows the systems under study. It reports the polymer's molecular weight, the number of available data, the experimental pressure and temperature ranges at the LCST loci, and the T_r and P_r referred to the critical T and P of the solvent. The data are grouped in the following mixtures: polymer + CO_2; polyolefines + hydrocarbons, polyacrilates, unique single systems and biopolymers.

It is worth to note the wide range of both: the temperature-pressure conditions and the polymer-solvent mixtures reported.

Table 1.
S-L parameters of the PFOMA and solubility parameters of the polymer-solvent.

PFOMA						CO_2	Ψ
MW	T^*, K	P^*, bar	ρ^*, g/cm^3	r	δ(MPa)$^{1/2}$		
110000	542.73	3408.2	1.659	5007.88	16.83	13.43$^+$	**1.57**

$^+$Experimental data (see Table 3).

At reduced conditions, however, it is observed that the LCST loci appear in the neighborhood of the solvent's critical point; around 0.6 to 1.2 of the pure solvent's reduced temperature. The molecular weight, in most of the cases, ensures that the θ point is found for the solutions at equilibrium. The authors have observed that molecular weight above 100,000 is sufficient to lie in the θ point proximity region.

Table 3 reports the mean values of the solubility parameter reported in the literature for a number of pure solvents, the corresponding predicted values using the S-L equation, and the percentage of error in the prediction. The error from the S-L equation is smaller than 2% in average. This value means that the prediction from the S-L equation is acceptable even for different temperatures as is shown for several substances. Table 3 includes the solubility parameter of diethyl ether because the uncertainty in the calculation of this parameter for DME (which is in the same family). As it is observed, the percentage error in the prediction for diethyl ether is smaller than that for the DME. The DME presents the larger prediction error from the S-L equation, this in spite of the data used for the adjustment were taken from recently reported experimental PvT data. It is possible that the deviation is due to the high polarity of the DME which in turn increases the solubility parameter. In the cases of the methyl and ethyl acetates (used also as reference), however, the predictions are quite close to those reported in the literature. These compounds possess a higher polarity than that for the DME. The S-L equation, according with our

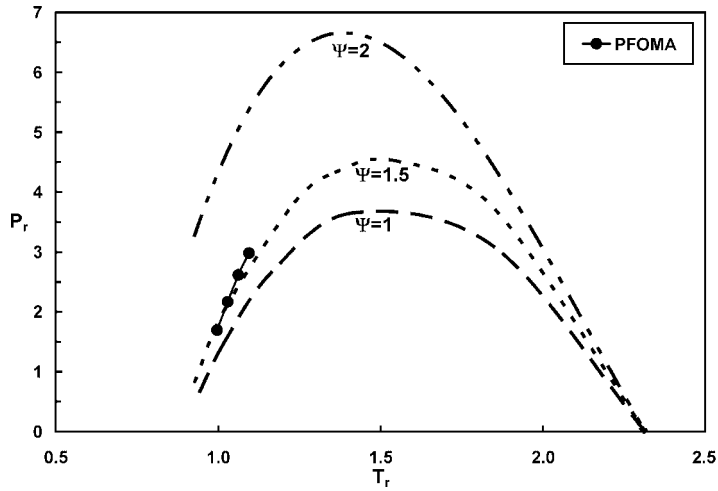

Figure 4.
LCST to reduced conditions of the PFOMA in supercritical CO_2, comparative to the simulation results Carlo Mounts to different Ψ.

Table 2.
Experimental information LCST conditions of polymers and biopolymers solutions in the supercritical region of the pure solvent.

System	N_d	$MW_{polymer}$, k	Range				Reference
			T, °C	P, bar	T_r	P_r	
PFOMA-CO_2	4	110	30–60	125–220	1.00–1.10	1.69–2.98	[51]
PFOA-CO_2	6	1,100	30–80	138–286	1.00–1.16	1.87–3.88	[52]
PFD-CO_2	7	2.5	35–100	89.6–208.9	1.01–1.23	1.21–2.83	[53]
PHDFDA-CO_2	4	254	25–100	115–331	0.98–1.23	1.56–4.49	[54]
PTAN-CO_2	7	NA	24–70	116.4–253.9	0.98–1.13	1.58–3.44	[55]
PE-nButane	10	420	141.25–192.15	260–305	0.98–1.09	6.84–8.03	[56]
PE-nPentane	6	121	147.85–200.85	131–196	0.90–1.01	3.89–5.82	[57]
PE-nHexane	12	52	162.55–221.87	20.24–97	0.86–0.98	0.67–3.22	[59]
PE-Isohexane	18	52	138.56–222.28	18.93–122.73	0.83–1.00	0.63–4.08	[59]
PE-nHeptane	5	125	190–230	20–71	0.86–0.93	0.73–2.59	[60]
PP-1Butene	7	197	90–150	20.27–130.5	0.87–1.01	0.50–3.25	[61]
PP-nButane	6	245	100–150	21.48–114.4	0.88–1.00	0.57–3.01	[61]
PP-nPentane	13	95.4–216	151.85–196.85	15.6–77	0.91–1.00	0.46–2.29	[57,62–63]
PIB-nButane	11	1,660	0–142	48.2–305.9	0.64–0.98	1.27–8.05	[64]
PIB-2MB	6	1,660	57.1–150	15.6–176.1	0.72–0.92	0.46–5.20	
PIB-nPentane	20	1,000–1,660	78.4–200	8.7–208	0.75–1.01	0.26–6.17	
PIB-nHexane	4	1,660	141.5–187.5	8–84.1	0.82–0.91	0.27–2.79	
PIB-nHeptane	6	1,000	170–220	13–83	0.82–0.91	0.47–3.03	[60]
PB-1Butene	9	1,280	133.38–172.04	102.2–164.7	0.97–1.06	2.54–4.10	[65]
POA-DME	8	100	51–179.7	25.9–222	0.81–1.13	0.49–4.24	[66]
POA-1Butene	4	100	120.8–179	46.6–132.8	0.94–1.08	1.16–3.30	
POA-nButane	5	100	100.5–180.2	29.3–139.7	0.88–1.07	0.77–3.68	
POA-Propylene	7	100	61.1–180.4	115.5–281	0.92–1.24	2.51–6.11	
POA-Propane	8	100	52.9–182	105.2–277.6	0.88–1.23	8.90–12.96	
PDA-DME	5	130	101.5–181.8	44.5–177.6	0.94–1.14	0.85–3.39	[67]
PDA-1Butene	4	130	121.9–181.7	53.5–139.7	0.94–1.08	1.33–3.48	
PDA-nButane	6	130	81.4–181.6	19–143.1	0.83–1.07	0.5–3.77	
PDA-Propylene	7	130	60.9–180.5	96.6–277.6	0.92–1.24	2.1–6.04	
PDA-Propane	7	130	58.9–180.4	169–285.9	0.90–1.23	10.40–13.15	
PNPMA-DME	5	480	102.2–183.1	36.9–200	0.94–1.14	0.70–3.82	[68]
PNPMA-1Butene	5	480	102.3–181.2	21.7–153.5	0.90–1.08	0.54–3.82	
PNPMA-nButane	5	480	101.1–181.7	60.3–170.7	0.88–1.07	1.59–4.49	
PNPMA-Propylene	7	480	60.3–180.8	115.5–322.4	0.91–1.24	2.51–7.01	
PNPMA-Propane	7	480	59.4–181.4	208.6–332.8	0.90–1.23	11.34–14.26	
PEHMA-DME	5	100	102.35–182.75	63.8–206.9	0.94–1.14	1.22–3.95	[69]
PEHMA-1Butene	5	100	101.55–182.25	29.3–150	0.89–1.09	0.73–3.73	
PEHMA-nButane	5	100	103.95–181.95	46.6–153.5	0.89–1.07	1.23–4.04	
PEHMA-Propylene	7	100	61.35–180.25	114.8–312.1	0.92–1.24	2.51–7.01	
PEHMA-Propane	7	100	62.45–181.15	143.1–301.7	0.91–1.23	3.37–7.10	
PEHA-DME	5	90	101.15–179.35	43.1–175.9	0.94–1.13	0.82–3.36	
PEHA-1Butene	4	90	121.25–179.95	43.1–129.3	0.94–1.08	1.07–3.22	
PEHA-nButane	5	90	100.55–180.25	23.5–141	0.88–1.07	0.62–3.71	
PEHA-Propylene	5	90	100.75–180.75	170.7–287.9	1.02–1.24	3.71–6.26	
PEHA-Propane	6	90	80.95–179.35	136.2–274.1	0.96–1.22	3.21–6.45	
PIPA-DME	5	120	100.1–179.3	41–181	0.93–1.13	0.78–3.45	[70]
PDMS-Propane	7	626	80.3–168.3	37.2–157.9	0.96–1.19	0.88–3.72	[64]
PDMS-nButane	4	626	136.6–176.7	29.7–82.1	0.96–1.06	0.78–2.16	[64]
PS-Cyclohexane	6	101	223.2–242	20.6–51	0.90–0.93	0.51–1.25	[71]
PS-Methylacetate	6	1,800	122.1–198.4	12.3–161.7	0.78–0.93	0.26–3.46	[72]
PMMA-HCFC22	9	74	70–150	58.7–303.3	0.93–1.15	1.18–6.10	[73]
PVDF-DME	5	200	86.1–187.7	25–312.5	0.90–1.15	0.48–5.96	[74]
D,L-PLA-DME	6	30	55.5–99.8	24.7–137.3	0.82–0.93	0.47–2.62	[75]
D,L-PLA-HCFC22	6	30	65.1–109.6	33.5–155.5	0.92–1.04	0.67–3.13	[76]
D,L-PLA-HFC134a	8	30	30.5–99.9	252.4–401.2	0.81–1.00	6.22–9.89	[76]
L-PLA-DME	9	230	59.65–138.45	63–249	0.83–1.03	1.20–4.75	[77]
L-PLA-HCFC22	13	230–300	50.15–136.55	36–261	0.88–1.11	0.72–5.25	[77–79]
PCL-DME	9	170	55.8–198.4	261.7–496.6	0.82–1.18	4.99–9.48	[80]
PCL-HCFC22	13	170	39.6–171.1	43.1–454.8	0.85–1.20	0.87–9.15	[80]

Nd, number of data points.

Table 3.
Calculation results of the solubility parameter of solvents with the S-L equation.

Component	Mean	Reference	S-L	%AAD	Reference
Propylene	13.41	[21,33,81]	12.75	4.93	[85]
Propane	12.97	[21,33,35,41,81]	12.35	4.82	[86]
1-Butene	13.81	[21,33,81]	14.17	−2.63	[64]
n-Butane	13.94	[21,32–33,35,37,41–42,82]	13.83	0.75	[86]
Pentane	14.38	[21,32–33,35,37,41,81]	14.44	−0.43	[87]
80 °C	13.46	[83]	12.78	5.04	
120 °C	11.27	[84]	11.21	0.57	
Isopentane	13.77	[21,33,35,81]	14.08	−2.26	[86]
n-Hexane	14.86	[21,32–33,35,37,41–42,81–82]	14.71	1.06	
80 °C	13.80	[83]	13.39	2.99	
120 °C	12.17	[84]	12.22	−0.38	
Isohexane	14.49	[33,41–42]	14.71	−1.49	
Cyclohexane	16.77	[21,32–33,35,37,41,81]	16.99	−1.29	
80 °C	15.60	[83]	15.65	−0.30	
120 °C	14.26	[84]	14.48	−1.55	
n-Heptane	15.19	[21,32–33,35,37,41,81]	15.18	0.01	
80 °C	14.07	[83]	13.97	0.74	
120 °C	12.84	[84]	12.91	−0.58	
CO_2	13.43	[33,41]	12.32	8.25	[87–88]
HCFC-22	14.93	[21,33,35]	14.63	2.02	[87–88]
DME	17.78	[21,33,35]	14.58	18.00	[89]
Diethyl ether	15.47	[21,32–33,35,41–42,82]	15.48	−0.01	[86]
Methyl acetate	19.15	[21,32–33,35,37,42]	19.28	−0.66	
80 °C	17.93	[83]	17.52	2.27	
120 °C	15.95	[84]	15.97	−0.11	
Ethyl acetate	18.38	[21,32–33,35,37,41–42,82]	18.14	1.28	
80 °C	16.79	[83]	16.49	1.79	
120 °C	15.10	[84]	15.03	0.47	
			Rel. Error	**1.55**	
			Abs. Error	**2.38**	

calculations, resulted in a suitable model for the prediction of the solubility parameter.

For polymers, Table 4 reports also the deviations of the predicted values from the S-L equation. There are additional polymers because in this way we have a better reference for the predictions. The relative average error is smaller than 1% which suggests an adequate prediction. However, there is an absolute average error of 6.4%. It is necessary to point that the magnitude of solubility parameters of polymers lies in an interval of values which is determined from an assortment of experimental techniques and groups of solvents. The solubility parameter of polymers is determined by indirect procedures; measuring the solubility of these macromolecules in a diversity of solvents and applying the Flory parameter χ (Eq. 4). Several experimental techniques such as the IGC (Inverse Gas Chromatography),[85–86,101–104] intrinsic viscosity measurement, density measurement are commonly used.

The S-L equation of state resulted in a suitable predictive model to determine solubility parameter of diverse solvents and polymers considered for study in this work. The calculated conformational parameter Ψ will provide therefore a close idea about the solution's behavior around the LCST loci from the S-L equation of state.

Results and Disscusion

Table 5 registers, for the experimental systems compiled in this work, the conformational parameter Ψ obtained from two sources: calculated with the S-L equation and from literature. It is evident that this parameter clarifies the

Table 4.
Calculation results of the solubility parameter of polymers with the S-L equation.

Polymer	Mean	Reference	S-L	%AAD	Reference
PE	16.45	[21,32–33,35–37,39,41–42]	19.47	−18.34	[86]
166 °C	17.75	[90]	17.59	0.88	
PP	17.87	[21,35–37,39]	16.18	9.44	[63]
PB	16.98	[39]	17.12	−0.82	[65]
PIB	15.96	[33,35–37,39,42,82]	17.37	−8.88	[86]
PS	19.50	[21,32–33,35–37,39,41–42,82,91]	19.19	1.57	
PDMS	16.41	[36–37,39,42]	15.28	6.87	
PMMA	21.92	[21,32–33,35–37,39,41–42,82,92]	21.25	3.04	[52]
PMA	20.45	[32,36–37,39]	20.64	−0.94	[86]
PEA	19.13	[33,36,39]	19.44	−1.61	[86]
PPA	18.50	[36]	21.00	−13.50	[96]
PNBA	19.39	[21,33,35–36]	20.85	−7.52	[96]
PEMA	19.55	[33,35–37,39,82,92]	19.63	−0.41	[86]
PBMA	18.59	[33,35–37,39,92]	19.07	−2.58	[86]
PVDF	23.23	[21]	17.79	23.42	[97]
PA	27.64	[21,32,35–37,41]	22.58	18.32	[86]
PVC	20.49	[21,32–33,35–37,39,41–42]	19.48	4.94	
PVAC	20.18	[21,32–33,35–37,39,41–42]	20.94	−3.77	
L-PLA	21.73	[93]	22.37	−2.94	[96]
DL-PLA	20.76	[94–95]	21.56	−3.87	[87]
PCL	20.20	[39]	20.29	−0.46	[86,98]
			Rel. Error	**0.14**	
			Abs. Error	**6.39**	

compatibility between the polymer and the solvent in the solution. For a fixed T and low values of Ψ, turning the polymer and solvent mutually compatible in the solution needs a relatively low pressure. As the parameter Ψ increases the solution's compounds become incompatible each other. As a consequence of this, the pressure must be increased in order to stabilize the solution and make the polymer soluble in the solvent. In these cases, the polymer-polymer and solvent-solvent molecular interactions are the dominant ones due to the polar nature of the strong interactions of the components in the mixture.

For the analysis of results it has been considered the polar interaction that some solvents or polymers present, the discussion is based on the Hansen's solubility parameter (HSP) that includes the polar character of the substance. Grouping the two polar terms (δ_p, polarity and δ_h, hydrogen bonds), being analyzed the contribution that these have on the parameter of solubility and in the compatibility of the studied systems in relation to Ψ. The polar contribution is evaluated in terms in the quadratic way of the equation (1).

$$\%\ \textit{polar contribution} = (\delta_p^2 + \delta_h^2) \Big/ \delta_o^2 * 100 \quad (15)$$

The graphs shown in the discussion section of this work the value of Ψ for each mixture is indicated in parenthesis. The values were determined using the solubility parameters reported in the literature. In the following, the analysis of each experimental system studied is presented.

Fluorinated Polymers in CO_2

Figure 5 presents P_r vs. T_r curves for polymers soluble in CO_2. It is observed that the LCST curves, for most of the systems studied, are located around $\Psi = 1.5$ in agreement with the molecular simulation results. The PFOMA is lightly more compatible than the PFOA which is indicated also from the values of their conformational parameter of 1.57 and 1.8, respectively (see details in Figure 5). The PHFDA and PTAN present similar beha-

Table 5.
Calculation of the conformational parameter, Ψ, for the studied mixtures.

System	$\Psi_{S\text{-}L}$	$\Psi_{lit.}$
PFOA-CO_2	2.13	1.80
PFOMA-CO_2	1.87	1.57
PFD-CO_2	1.48	1.25
PDMS-CO_2	1.54	1.45
PE-nButane	1.98	1.39
PE-nPentane	1.82	1.31
PE-Isohexane	1.75	1.29
PE-nHexane	1.75	1.22
PE-nHeptane	1.28	1.08
PP-nButane	1.37	1.67
PP-1Butene	1.30	1.71
PP-nPentane	1.26	1.57
PIB-nButane	1.58	1.31
PIB-2MB	1.52	1.34
PIB-nPentane	1.45	1.23
PIB-nHexane	1.15	1.15
PIB-nHeptane	1.14	1.05
PB-1Butene	1.46	1.51
POA-Propane	1.96	1.77
POA-Propylene	1.83	1.66
POA-nButane	1.56	1.54
POA-1Butene	1.49	1.56
POA-DME	1.40	0.94
PDA-Propane*	1.88	1.71
PDA-Propylene	1.77	1.60
PDA-nButane	1.50	1.48
PDA-1Butene	1.43	1.51
PDA-DME	1.35	0.91
PDMS-Propane	1.53	1.56
PDMS-nButane	1.22	1.35
PS-Cyclohexane	1.13	1.15
PS-Methyl acetate	0.99	1.02
PMMA-HCFC22	2.11	2.11
PVDF-DME	1.49	1.71
D,L-PLA-DME	2.19	1.36
D,L-PLA-HCFC22	2.17	1.93
D,L-PLA-HFC134a	2.58	2.39
L-PLA-DME	2.35	1.49
L-PLA-HCFC22	2.34	2.12
PCL-DME	1.94	1.29
PCL-HCFC22	1.92	1.83

*Parameters S-L of PDA[104]

vior. For this pair there is not information available about their solubility parameter, however, are both fluorinated polymers that exhibit compatibility with supercritical CO_2.[54,55] For the PFD the curve lies below the corresponding one for the calculated conformational parameter (around 1.3-1.5). This is because the experimental values for a molecular weight of 2500 do not correspond to the LCST curve at the θ point. It can be expected that as the molecular weight is increased, the curve moves up to a high pressure region; in the zone of the fluorinated polymers. The experimental data, however, are useful to show the relevance of the molecular simulation results.

Polyolefins with Hydrocarbon Solvents C_4 – C_7

For polyethylene solutions a favorable effect in solubility can be observed as the carbon number of solvent increases. This tendency is observed in both: the LCST curve behavior and the magnitude of Ψ (see Figure 6). Albeit the PE-heptane the LCST lies lightly above the corresponding curve for the PE-hexane, -contrary to the expected behavior since the hexane's solubility parameter is smaller than the one for the heptane- the discrepancy obeys mainly to the fact that the molecular weight of PE en the mixture with hexane is reported as 52,000 (to the similar with the iso-hexane) and this is not sufficient enough to reach the θ point conditions. The molecular weight of PE in the mixture with heptane is reported as 125,000 which ensure the θ point conditions. The LCST curves for the mixtures of PE with either hexane or iso-hexane at the θ point would migrate to higher pressure regions, producing in this way, a better congruency with the expected results.

The conformational parameter calculated from the S-L equation deviates from that obtained from literature data (see Table 5) the equilibrium is obtained at larger Ψ with respect to the molecular simulation results. This is, perhaps, because the polyethylene possesses a small polar contributions to the solubility parameter ($\delta_d = 16$, $\delta_p = 0.8$, $\delta_h = 2.8$)[21] but this contribution in hydrocarbons is null. This small difference may produce a deviation in the polymer solubility so a larger pressure is required to homogenize the solution. The Ψ values from the S-L equation are larger than those obtained from experimental data. This is in agreement with the simulation results.

For the polyisobutylene mixtures (see Figure 7) the tendencies are similar than

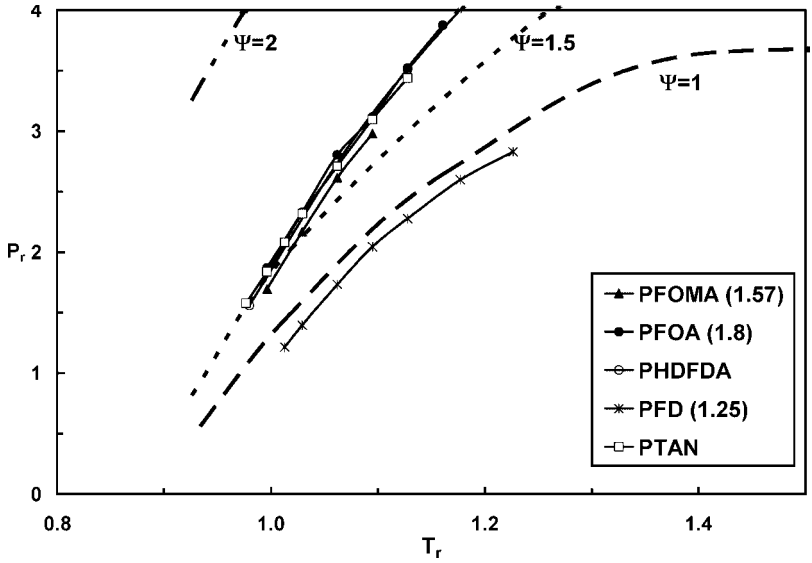

Figure 5.
Experimental LCST curves to reduced conditions of the pure solvent. Mixtures of fluorinated polymer-supercritical CO_2 in comparison with molecular simulation in Ψ terms.

those obtained from molecular simulation. However, the deviations are larger considering the Ψ values. In this case, the polyisobutylene presents appreciable contributions of both: polarity and hydrogen bonds: ($\delta_d = 14.5$, $\delta_p = 2.5$, $\delta_h = 4.7$)[33,35,82] in comparison to polyethylene. The polar contribution to the solubility parameter amounts the 12% of total. This polar contribution is reflected in the LCST curve's displacement to a high pressure in order to compatibilize the solutions despite of larger polyethylene solubility was expected. In both, the PE and PIB cases, the polymer-polymer molecular interactions are dominant in the mixture behavior.

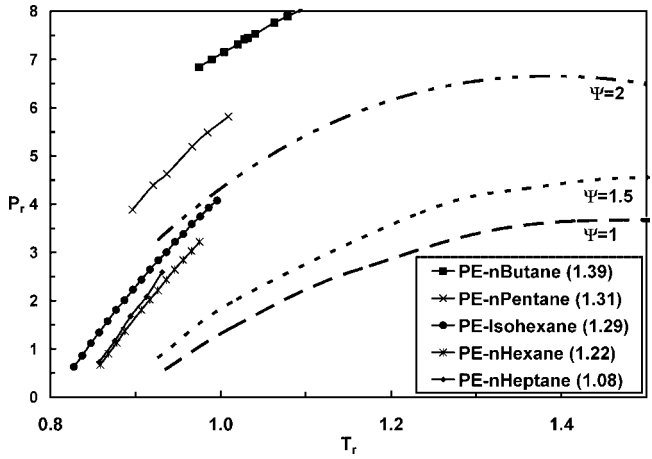

Figure 6.
Reduced LCST of polyethylene-hydrocarbon solvent C_4-C_7.

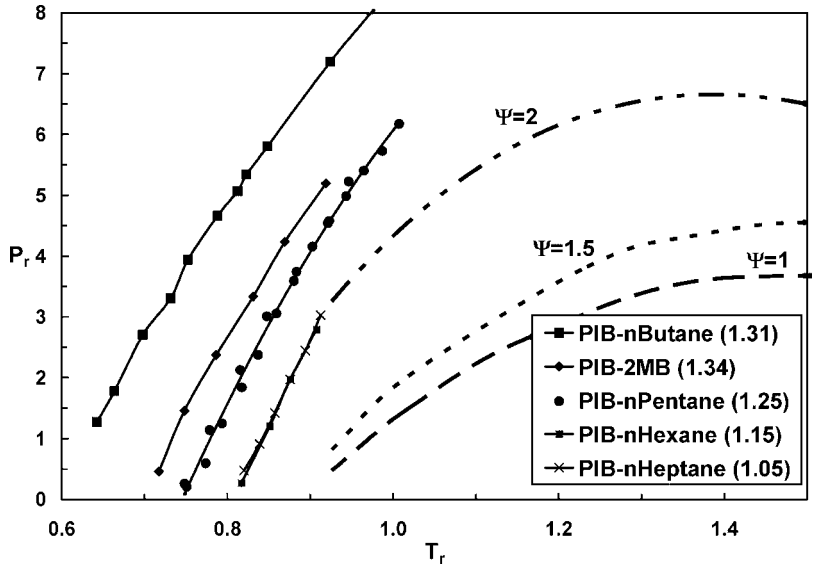

Figure 7.
Reduced LCST of polyisobutylene-hydrocarbon solvent C4-C7.

This make the LCST curves to be displaced to high pressures so the stability of the solution is reached.

For the polypropylene ($\delta_d = 18.0$, $\delta_p = 0.0$, $\delta_h = 1.0$)[21] the polar contribution is essentially null with a solubility parameter greater than those for polyethylene and polyisobutylene (18.04 vs. 16.44 and 15.96 respectively). It is expected, therefore, LCST curves in the high Ψ value

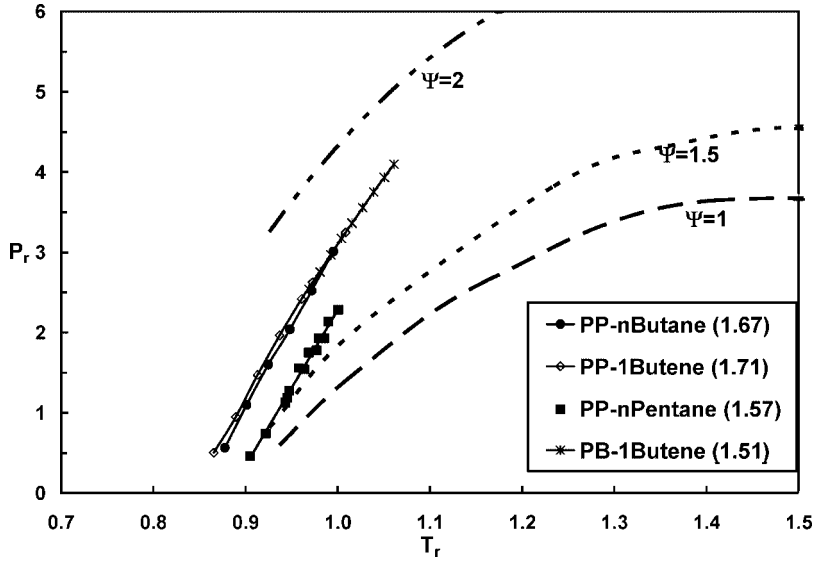

Figure 8.
Reduced LCST of polypropylene-hydrocarbon solvent C_4-C_5.

region. However since the polar contributions are not significant, the LCST curve behavior are quite similar to the molecular simulation results as well as the Ψ calculated from literature data (see Table 5). Observe how Ψ calculated from simulation are in agreement with experimental data. In the polybutene + 1-butene mixture the LCST curve behavior is similar to that of polypropylene.

Although the solubility parameter relationship is a simple reference, it results in a strong support about the analysis of the polymeric solutions behavior in the critical region of the pure solvent. In addition, the molecular simulation results reflect the tendencies of the experimental LCST curves.

Polyacrylates

To carry out a comparative of the experimental data of the systems studied (POA and PDA) and the molecular simulation, were estimated the solubility parameters of these polymers, since don't have the data. For poly-(alkyl acrylates) and poly-(alkyl metacrylates) the solubility parameters were correlated with the carbon number of the alkyl group using available literature data. In the Figure 9 the correlations are shown so much for the poli(alquil acrilatos) as poli(alquil metacrilatos) this last one used as reference.

Using these correlations, the solubility parameters of the linear poly-(alkyl acrylates) POA and PDA were estimated resulting in 17.3 and 17 respectively. The solubility parameter curve for the linear poly-(alkyl metacrylates) derivatives shows similitude in the data for both polyacrylates. The descendent behavior of the curve as an effect of the same alkyl radical growth in the polymeric chain is confirmed in Figures 9a and 9b.

Figure 10 depicts the results for the POA with different hydrocarbon solvents and DME. Surprisingly, the molecular simulation reproduces the experimental data tendencies quite well even though the acrylic polymers have strong polar contributions which influence the solubility behavior. For example: the poly-(butyl acrylate) ($\delta_d = 16.2$, $\delta_p = 9.0$, $\delta_h = 3.0$)[21] has a polar contribution of 25%, the poly-(ethyl metacrylate) ($\delta_d = 17.6$, $\delta_p = 9.7$, $\delta_h = 4.0$)[33] of 26% and the PMMA ($\delta_d = 18.1$, $\delta_p = 10.5$, $\delta_h = 15.1$)[21] of 29%.

Tendencies about the solvent strength for the different compounds are in agreement with Ψ. The increase in its value displaces the LCST curves to high pressures. The order in the solubility strength, from low to high is: propane < propylene < n-butane < 1-butene < DME. The solvent strength of 1-butene is improved by its polar contribution ($\delta_d = 13.2$, $\delta_p = 1.3$, $\delta_h = 3.9$)[21] which effects lightly its role as solvent (9% polar) with respect to its solubility parameter comparatively to n-butane. This is observed in the Figure 10. Exceptionally in the case of the mixture POA-DME, the LCST curve is located to more pressures of that waited according to the solubility parameter of the DME and Ψ comparative with the experimental behavior. Ψ indicates a good compatibility of the polymer and therefore low pressures to solvate the polymeric chains. However, this is not completely true. It seems that the polar contributions of the solubility parameter of DME ($\delta_d = 15.2$, $\delta_p = 6.1$, $\delta_h = 5.7$)[21] representing the 23% of total, are in competence with the polar contributions of the poly-(alkyl acrylates). This competence promotes the polymer-polymer and the solvent-solvent interactions in detriment of the polymer-solvent interactions, bringing about a displacement of the mixture compatibility and therefore higher pressure are needed to reach the solubility. This is reflected in the solution behavior when the LCST curve is located a larger Ψ.

The conformational parameters Ψ calculated from the molecular simulation, from literature data and from the S-L equation are similar. In the Figure 10 the LCST curve for the PIPA+DME mixture is shown. Identical to the previous cases, the curve shows a reproducible behavior from the molecular simulation results.

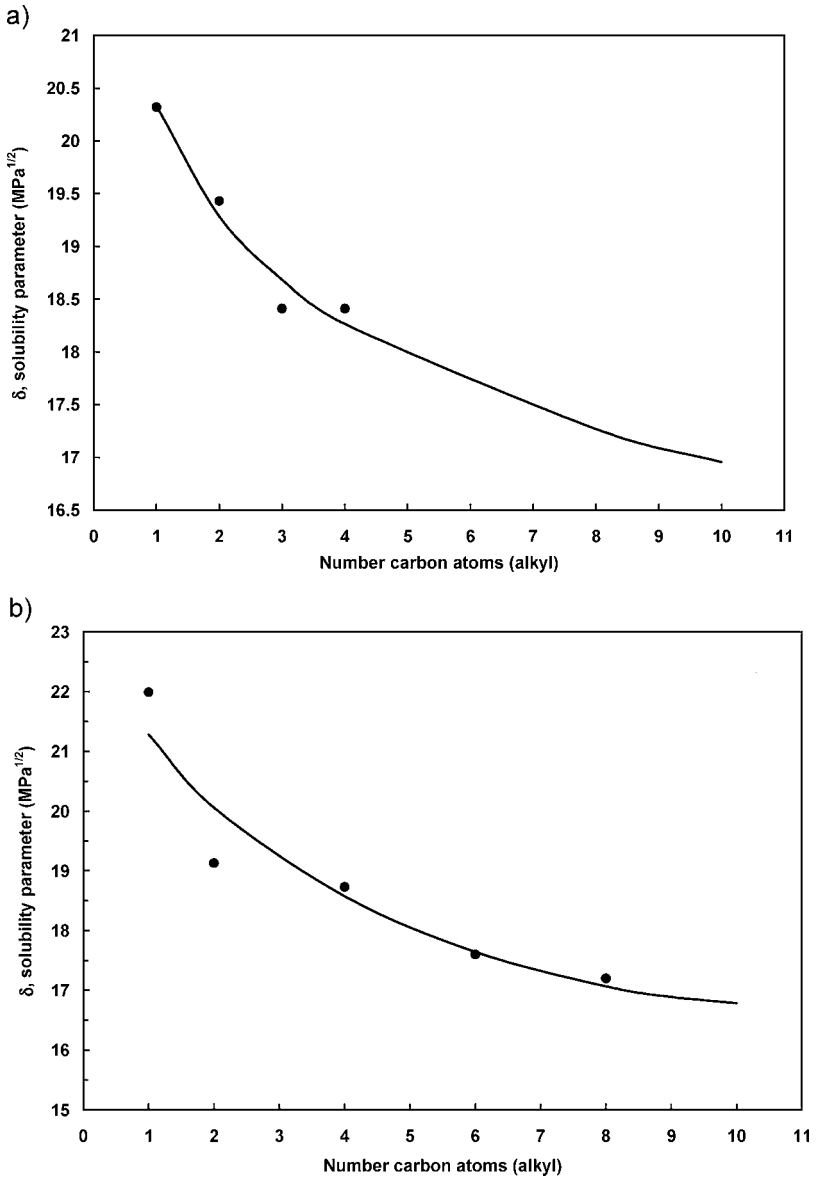

Figure 9.
Effect of the carbon number of the alkyl group number of atoms of carbon in the parameter of solubility of the poly-(alkyl acrylates) (a) and poly-(alkyl metacrylates) (b).

Figure 11 depicts the LCST curves for the PDA mixtures. The molecular simulation results adequately adjust the experimental data, following the right tendency with the effect of Ψ. In this case also, the mixtures PDA + 1-butene and PDA + DME behave similar than the POA mixture, corroborating the previously observed.

Figure 12 shows the LCST curves for the rest of the poly-(alkyl acrylates) and poly-(alkyl metacrylates) mixtures. All of them depict a tendency which is equivalent to those already analyzed. Even though the solubility parameters of the polymers are not available it is expected that all of them exhibit a similar behavior which is also

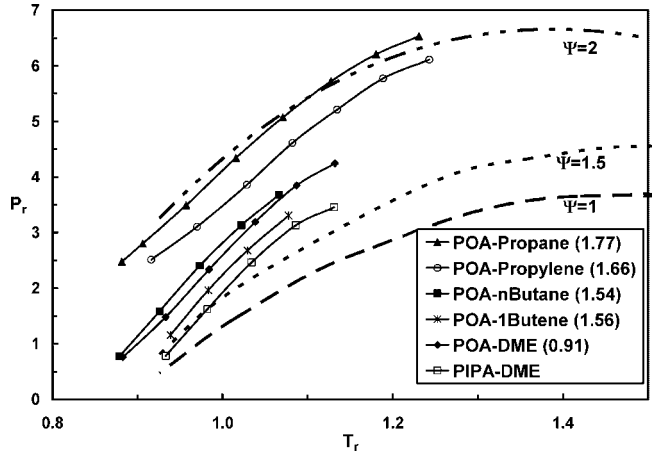

Figure 10.
Reduced LCST of POA-solvent and PIPA-DME.

present in the case of fluorinated polymers with CO_2.

The same as in the previous cases, the solubility parameters provide an assertive reference for the polymeric mixture behavior in the supercritical region of the pure solvent. On the other hand the simulation results replicate the LCST curves of the polyacrylate mixtures.

Other Mixtures

Systems where the polar contributions influence the mixture behavior are presented. Figure 13 depicts different solutions having this kind of behavior, mainly with the PS, PMMA and PVDF polymers. In the PDMS case, where the polar effects are less significant with solvents with no polar contribution, the molecular simulation results and Ψ are congruent with the experimental data. Instead, for the other cases, a strong effect is observed possibly influenced by the molecular interaction between the polymer and solvent.

For the polystyrene ($\delta_d = 18.5$, $\delta_p = 4.5$, $\delta_h = 2.9$)[21] (polar contribution 8%) sys-

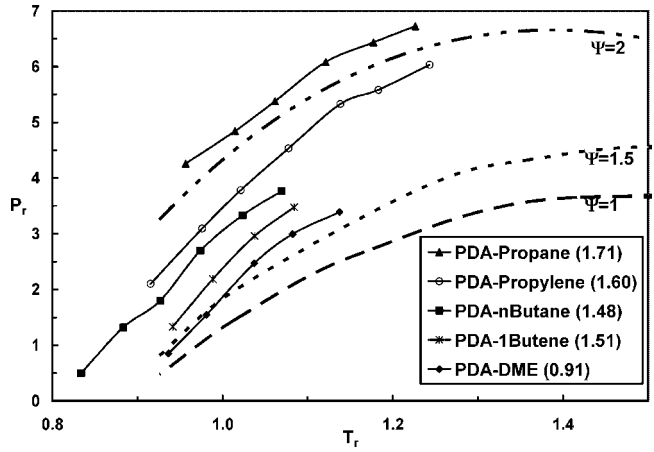

Figure 11.
Reduced LCST of PDA-solvent.

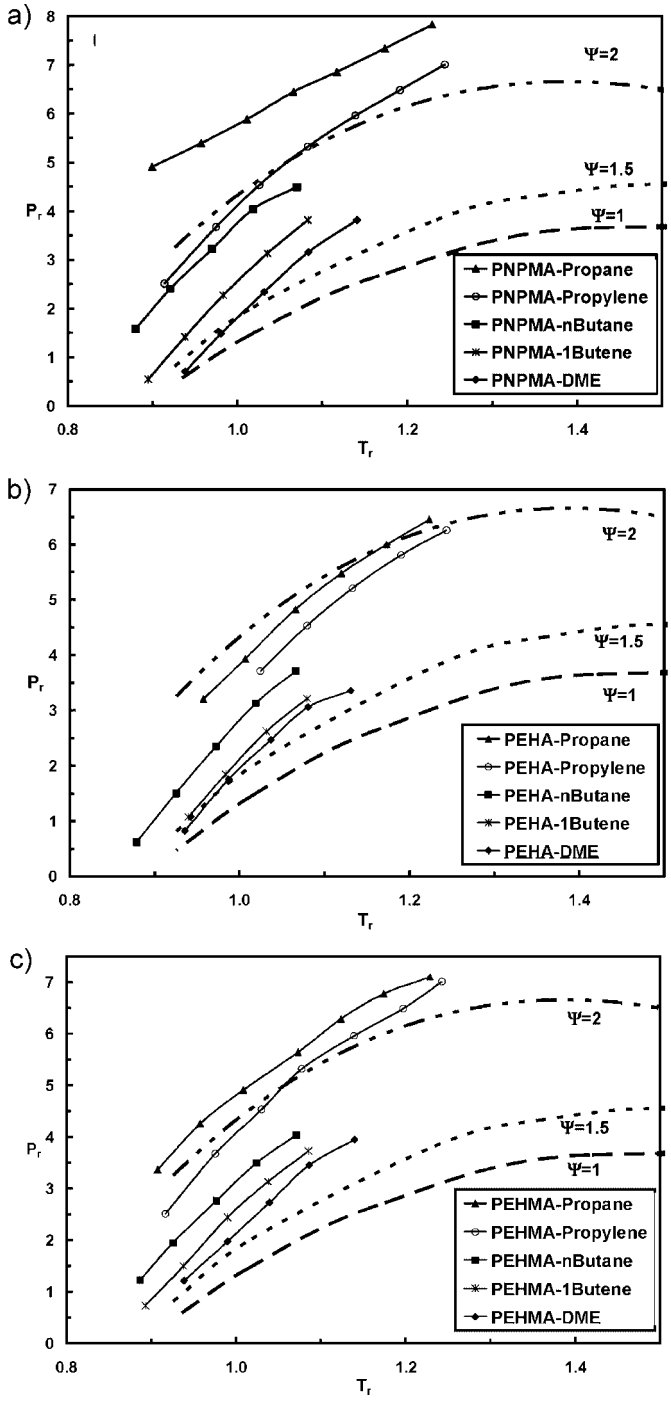

Figure 12.
Reduced LCST of PNPMA (a), PEHA (b) y PEHMA (c) with different solvents.

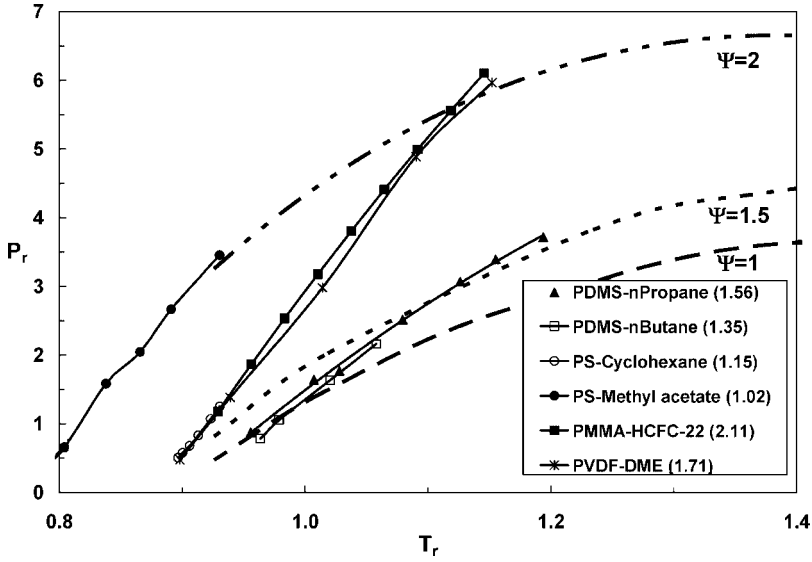

Figure 13.
Reduced LCST of different polymeric solutions.

tems it is observed that in the mixture with cyclohexane the polarity of PS does not influence the solution's behavior. In this case the cyclohexane does not exhibits polar effects. On the other hand, the mixture PS + methyl acetate is strongly affected by the polar contributions of acetate ($\delta_d = 15.5$, $\delta_p = 7.2$, $\delta_h = 7.6$),[21] (polar contribution of 31%). In this way the polymer-polymer and solvent-solvent interactions become dominant and therefore high pressure is required in order to solvate the PS.

For the PMMA + HCFC22 mixture the effect is contrary to the one presented by the PS + methyl acetate mixture. In this case the polar contributions of PMMA ($\delta_d = 18.1$, $\delta_p = 10.5$, $\delta_h = 15.1$,[21] polar contribution of 29%) and HCFC22 ($\delta_d = 12.3$, $\delta_p = 6.3$, $\delta_h = 5.7$,[21] polar contribution of 32%) are similar. The equilibrium between the intermolecular forces compensates the favorable interactions that improve the compatibility of the solution even though its behavior is reflected by the LCST curve appearance. It is observed that the Ψ relationship is being modified at the T_r and P_r conditions, evolving from 1.5 to 2. The same behavior is present with the mixture PVDF + DME [PVDF ($\delta_d = 17.0$, $\delta_p = 12.1$, $\delta_h = 10.2$ polar contribution of 46%) and DME ($\delta_d = 15.2$, $\delta_p = 6.1$, $\delta_h = 5.7$ polar contribution of 23%].[21] The strong molecular interactions influence, similarly, in the solution's behavior.

Biopolymers

In the biopolymer solutions the polar effects are important regarding the solution's behavior. This is confirmed mainly in the mixtures with DME which exhibit large deviations. Figure 14 depicts the results for the three biopolymers under study.

It is evident that the polar contributions to the solubility parameter influence strongly in the solutions' behavior. Mixtures with high values of Ψ are presented for this type of systems, excepting with DME where the magnitudes of Ψ are in the order of the previously studied mixtures.

Let's analyze the case of mixtures with the biopolymer L-PLA. The Table 6 presents, for L-PLA, DME and HCFC-22, the Hansen's solubility parameter (HSP), the dipole moment and the critical density. For these compounds the polar contributions are relatively high. For L-PLA is 27.5%

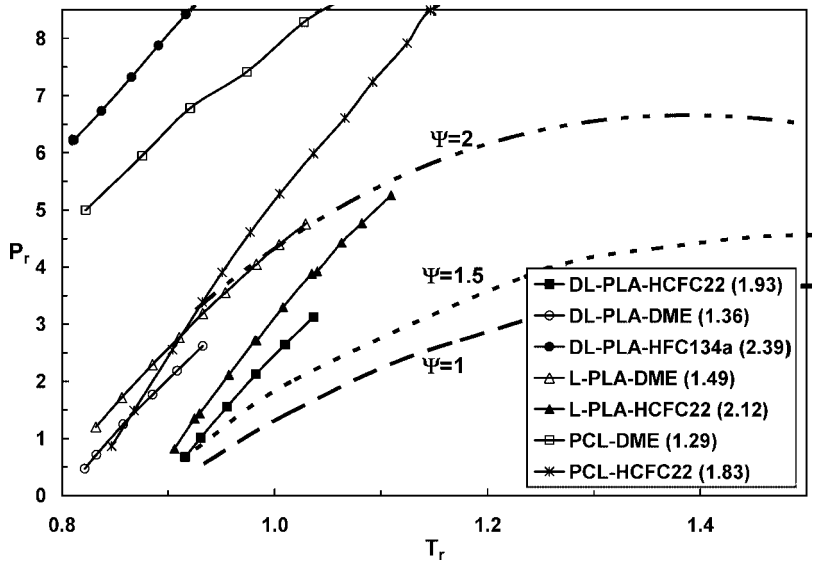

Figure 14.
Reduced LCST of biopolymeric solutions.

Table 6.
Properties of L-PLA, DME y HCFC-22.

Component	HSP, $MPa^{1/2}$				ρ_c, g/cm^3	$\alpha^{*}10^{25}$, cm^3	μ, D	Other interactions
	δ_d	δ_p	δ_h	δ_o				
L-PLA	18.5	9.7	6	21.73	–	–		
DME	15.2	6.2	5.7	17.34	0.258	52.2	1.3	H bonds
HCFC-22	12.3	6.3	5.7	14.95	0.522	44.4	1.4	H bonds

References: solubility parameter: L-PLA[93]; DME and HCFC-22[21]; others properties[80]

and, as mentioned above, for DMA the polar contribution is 23% meanwhile for the HCFC-22 this contribution is greater than 32%. It is observed that the behavior of the LCST curves is dominated by the polar forces of the components, for the Ψ calculated from the solubility parameters move away from the experimental curves. Even, the LCST curves for the biopolymer + DME and + HCFC-22, are contrary to those expected. The solubility strength of DME referred to its solubility parameter is higher than expected, however the experimental results indicate the contrary for all the biopolymer mixtures under study.

It is observed, from Table 6, that the polarity and dipolar moment of DME and HCFC-22 are quite similar, it is possible that the solubility strength of the HCFC-22 is high because its critical density is large in comparison to that of the DME. This provides the HCFC-22 with a better solvency power, in addition to its polar nature, to solvate biopolymer chains. Contrary to the HCFC-22, the DME with low critical density requires higher pressures.

Similar results are presented for the other two biopolymers (PCL and D,L-PLA) where the LCST curves of the systems with -DME and -HCFC-22 is contrary with regard to the calculated Ψ value, again the solvency power of the HCFC-22 stabilizes the biopolymeric solutions comparatively to smaller pressures when the solvent is the DME. In all the cases the high effect of polar interaction of

the systems is shown (to also see the system DL-PLA-HFC134a in the Figure 14).

It is worth to note that for all polymer + DME mixtures under study in this work, the solubility parameter of DME, in the literature data, seems to be overestimated. It would be interesting to perform a study about this topic.

Conclusions

It has been proved the utility of molecular simulation in the knowledge and analysis of the polymeric chain collapse in a supercritical solvent at the limits of LCST curve in the θ point. For the very first time the conformational parameter Ψ is proposed as the ratio of the structure-energy interactions between the polymer and the solvent. This parameter defines the behavior of these mixtures at the supercritical region of the pure solvent and it has been widely verified with experimental data which confirm its application.

Ψ has been related to the solubility parameters of both polymer and solvent using the simulation results reported in part 1 and has been analyzed with experimental data. In most of the cases, the tendencies in the behavior of the experimental systems are similar to those obtained from simulation, with the solubility parameter as an important support to characterize the compatibility of the mixtures. Mixtures with large Ψ exhibit their LCST curves displaced to high pressures and this comportment is related with the difference between the solubility parameters of the polymer and the solvent. On the contrary, when Ψ approaches 1.0, the LCST curves are displaced to lower pressures, in agreement with the simulations and evidenced with the experimental data.

It was observed that the polar contributions of both the solvent and the polymer alter the behavior of the solutions. They put in evidence, for some cases, the influence of the dominant polymer-polymer and solvent-solvent interactions that deviates the stability to larger pressures than those expected. On the other hand, for systems where the polymer-solvent interaction is the dominant one, the stability of the solution is reached at lower Ψ. In this aim, the Hansen's solubility parameter (HSP) has been used to relate the polar contribution with the solution behavior.

Finally, the experimental evidence is a clear indication that for these systems the equilibrium near to the solvent's supercritical conditions is adequately represented through the analysis by molecular simulation, extended to reduced conditions by mean of the conformational parameter Ψ. The relationship structure-energetic interaction between the polymer and the solvent -generalized by the employment of the solubility parameter- proves that this kind of systems can be analyzed in the view of thermodynamic fundamentals supported with the application of a suitable model such as the S-L equations of state.

Nomenclature

2MB	2, Methyl butane
CO_2	Carbon dioxide
DME	Dimethyl ether
HCFC22	Chlorodifluoromethane
HFC134a	1,1,1,2-Tetrafluoroethane
D,L-PLA	Poly(D,L-lactide)
L-PLA	Poly(L-lactide)
PA	Polyacrylonitrile
PB	Polybutene
PBMA	Poly(butyl methacrylate)
PCL	Poly(ε-caprolactone)
PDA	Poly(decyl acrylate)
PDMS	Poly(dimethylsiloxane)
PE	Polyethylene
PEA	Poly(ethyl acrylate)
PEHA	Poly(2-ethylhexyl acrylate)
PEHMA	Poly(2-ethylhexyl methacrylate)
PEMA	Poly(ethyl methacrylate)
PFD	Perfluoropoly-ether diamida
PFOA	Poly(1,1-dihydroperfluorooctylacrylate)
PFOMA	Poly(1H,1H-perfluorooctyl methacrylate)

PHDFDA	Poly(heptadecafluoro-decyl acrylate)
PIB	Polyisobutylene
PIPA	Poly[isopropyl acrylate]
PMA	Poly(methyl acrylate)
PMMA	Poly(methyl methacrylate)
PNBA	Poly(n-butyl acrylate)
PNPMA	Poly(neopentyl methacrylate)
POA	Poly[octyl acrylate]
PP	Polypropylene
PPA	Poly(propyl acrylate)
PS	Polystyrene
PTAN	Poly(1,1,2,2-tetrahydroperfluorodecyl acrylate)
PVAC	Poly(vinyl acetate
PVC	Poly(vinyl chloride)
PVDF	Poly(vinylidene fluoride)

[1] M. A. McHugh, V. J. Krukonis, *Supercritical Fluid Extraction. Principles and Practice*, 2nd Butterworth-Heinemann, **1994**.
[2] S. Kim, Y.-S. Kim, S.-B. Lee, Phase behaviors and fractionation of polymer solutions in supercritical carbon dioxide. *Journal of Supercritical Fluids* **1998**, *13*(1–3), 99–106.
[3] K. P. Johnston, Block copolymers as stabilizers in supercritical fluids. *Current Opinion in Colloid & Interface Science* **2000**, *5*(5–6), 351–356.
[4] P. L. Beltrame, A. Castelli, E. Selli, A. Mossa, G. Testa, A. M. Bonfatti, A. Seves, Dyeing of cotton in supercritical carbon dioxide. *Dyes and Pigments* **1998**, *39*(4), 335–340.
[5] G. Tepper, N. Levit, Polymer deposition from supercritical solutions for sensing applications. *Ind. Eng. Chem. Res.* **2000**, *39*(12), 4445–4449.
[6] Y. Wang, D. Wei, R. Dave, R. Pfeffer, M. Sauceau, Extraction and precipitation particle coating using supercritical CO_2. *Powder Technology* **2002**, *127*(1), 32–44.
[7] A. I. Cooper, Polymer synthesis and processing using supercritical carbon dioxide. *Journal of Materials Chemistry* **2000**, *10*(2), 207–234.
[8] J.-Y. Lee, B. Tan, A. I. Cooper, CO_2-in-Water emulsion-templated poly(vinyl alcohol) hydrogels using poly(vinyl acetate)-based surfactants. *Macromolecules* **2007**, *40*(6), 1955–1961.
[9] H. Yuvaraj, H. S. Hwang, M. H. Woo, E. J. Park, H. S. Ganapathy, Y.-S. Gal, K. T. Lim, Dispersion polymerization of styrene in supercritical CO_2 stabilized by random copolymers of 1H,1H-perfluorooctyl methacrylate and 2-dimethylaminoethyl methacrylate. *Journal of Supercritical Fluids* **2007**, in press.
[10] J. Jung, M. Perrut, Particle design using supercritical fluids: Literature and patent survey. *Journal of Supercritical Fluids* **2001**, *20*(3), 179–219.
[11] E. Reverchon, G. Caputo, I. De Marco, Role of phase behavior and atomization in the supercritical antisolvent precipitation. *Ind. Eng. Chem. Res.* **2003**, *42*(25), 6406–6414.
[12] S.-D. Yeo, E. Kiran, Formation of polymer particles with supercritical fluids: A review. *Journal of Supercritical Fluids* **2005**, *34*(3), 287–308.
[13] E. Reverchon, G. Della Porta, I. De Rosa, P. Subra, D. Letourneur, Supercritical antisolvent micronización of some biopolymers. *Journal of Supercritical Fluids* **2000**, *18*(3), 239–245.
[14] K. Matsuyama, K. Mishima, K.-I. Hayashi, H. Ishikawa, H. Matsuyama, T. Harada, Formation of microcapsules of medicines by the rapid expansion of a supercritical solution with a nonsolvent. *J. Applied Polymer Science* **2003**, *89*(3), 742–752.
[15] J. Fages, H. Lochard, J.-J. Letourneau, M. Sauceau, E. Rodier, Particle generation for pharmaceutical applications using supercritical fluid technology. *Powder Technology* **2004**, *141*(3), 219–226.
[16] E. Reverchon, R. Adami, Nanomaterials and supercritical fluids. *Journal of Supercritical Fluids* **2006**, *37*(1), 1–22.
[17] P. I. Freeman, J. S. Rowlinson, Lower critical points in polymer solutions. *Polymer* **1960**, *1*, 20–26.
[18] M. L. O'Neill, Q. Cao, M. Fang, K. P. Johnston, S. P. Wilkinson, C. D. Smith, J. L. Kerschner, S. H. Jureller, Solubility of homopolymers and copolymers in carbon dioxide. *Ind. Eng. Chem. Res.* **1998**, *37*(8), 3067–3079.
[19] J. Hildebrand, R. L. Scott, *Regular Solutions*, Prentice Hall, New Jersey, EUA 1962.
[20] A. F. M. Barton, Applications of Solubility Parameters and Other Cohesion Parameters in Polymer Science and Techology. *Pure & Appl. Chem.* **1985**, *57*(7), 905–912.
[21] C. M. Hansen, *Hansen Solubility Parameters: A User's Handbook*, CRC, Boca Raton, Florida 2000.
[22] S. Mandal, V. G. Pangarkar, Development of copolymer membranes for pervaporative separation of methanol from methanol-benzene mixture: a solubility parameter approach. *Separation and Purification Technology* **2003**, *30*(2), 147–168.
[23] F. E. Eichie, R. S. Okor, R. Groning, Application of solubility parameters to the formulation of acrylate methacrylate film coating systems. *Journal of Applied Polymer Science* **2003**, *87*(8), 1339–1344.
[24] C. M. Hansen, 50 Years with Solubility Parameters-Past and Future. *Progress in Organic Coatings* **2004**, *51*(1), 77–84.
[25] C. M. Hansen, Polymer Additives and Solubility Parameters. *Progress in Organic Coatings* **2004**, *51*(2), 109–112.

[26] D. Karst, Y. Yang, Using the Solubility Parameter to Explain Disperse Dye Sorption on Polylactide. *Journal of Applied Polymer Science* **2005**, *96*(2), 416–422.
[27] J. Liu, T. Liu, S. Kumar, Effect of Solvent Solubility Parameter on SWNT Dispersion in PMMA. *Polymer* **2005**, *46*(10), 3419–3424.
[28] W. Ma, J. Yu, J. He, Stability of Crystal forms of Syndiotactic Polystyrene Correlated with their Formation in Different Media Having Different Solubility Parameters. *Polymer* **2005**, *46*(24), 11104–11111.
[29] W. Ma, J. Yu, J. He, D. Wang, Stability of Form II of Syndiotactic Polypropylene Confirmed by Cold and Melt Crystallization in Supercritical Carbon Dioxide. *Polymer* **2007**, *48*(6), 1741–1748.
[30] Y. H. Lang, Z. M. Cao, X. Jiang, Prediction of Solvents Extraction-the Organochlorine Pesticides in Soil Using Solubility Parameter. *Talanta* **2005**, *66*(1), 249–252.
[31] C. M. Hansen, A. L. Smith, Using Hansen Solubility Parameters to Correlate Solubility of C60 Fullerene in Organic Solvents and in Polymers. *Carbon* **2004**, *42*(8–9), 1591–1597.
[32] A. F. M. Barton, Solubility Parameters. *Chemical Reviews* **1975**, *75*(6), 731–753.
[33] A. F. M. Barton, *CRC Handbook of Solubility Parameters and Other Cohesion Parameters*, CRC Press, Boca Raton, Florida 1983.
[34] K. L. Hoy, Tables of Solubility Parameters. Solvents & Coatings Materials Research & Development Department. Union Carbide Corporation, South Charleston, **1985**.
[35] J. Brandup, E. Immergut, *Polymer Handbook*, Third Edition, John Wiley & Sons, New York **1989**.
[36] D. W. Van Krevelen, *Properties of Polymers Their Correlation with Chemical Structure; Their Numerical Estimation and Prediction from Additive Group Contributions*, 3rd. Edition, Elsevier Science Publishers B.U, Amsterdam **1990**.
[37] G. Wypych, *Handbook of Solvents*, ChemTec Publishing, Toronto **2001**.
[38] C. Panayiotou, Solubility Parameters Revisted: An Equation-of-State Approach for its Estimation. *Fluid Phase Equilibria* **1997**, *131*(1–2), 21–35.
[39] L. A. Utracki, R. Simha, Statistical thermodynamics predictions of the solubility parameter. *Polymer International* **2004**, *53*(3), 279–286.
[40] E. K. Goharshadi, M. Hesabi, Estimation of Solubility Parameter Using Equations of State. *J. Molecular Liquids* **2004**, *113*(1–3), 125–132.
[41] E. Stefanis, I. Tsivintzelis, C. Panayiotou, The Partial Solubility Parameters: An Equation-of-State Approach. *Fluid Phase Equilibria* **2006**, *240*(2), 144–154.
[42] M. Hamedi, R. P. Danner, Prediction of solubility parameters using the group-contribution lattice-fluid theory. *Journal of Applied Polymer Science* **2001**, *80*(2), 197–206.
[43] T. J. Sheldon, C. S. Adjiman, J. L. Cordiner, Pure component properties from group contribution: Hydrogen-bond basicity, hydrogen-bond acidity, Hildebrand solubility parameter, macroscopic surface tension, dipole moment, refractive index and dielectric constant. *Fluid Phase Equilibria* **2005**, *231*(1), 27–37.
[44] L. Zhao, P. Choi, Study of the Correctness of the Solubility Parameters Obtained from Indirect Methods by Molecular Dynamics Simulation. *Polymer* **2004**, *45*, 1349–1356.
[45] S. R. Allada, Solubility Parameters of Supercritical Fluids. *Ind. Eng. Process Des. Dev.* **1984**, *23*(2), 344–348.
[46] L. L. Williams, J. B. Rubin, H. H. Edwards, Calculation of Hansen Solubility Parameter Values for a Range of Pressure and Temperature Conditions, Including the Supercritical Fluid Region. *Ind. Eng. Chem. Res.* **2004**, *43*(16), 4967–4972.
[47] Y. Marcus, Are solubility parameters relevant to supercritical fluids? *Journal of Supercritical Fluids* **2006**, *38*(1), 7–12.
[48] J. M. Prausnitz, R. N. Lichtenthaler, E. G. de Azevedo, *Molecular Thermodynamics of Fluid-Phase Equilibria*, Prentice Hall, New Jersey 1999.
[49] I. C. Sanchez, R. H. Lacombe, An elementary molecular theory of classical fluids. Pure fluids. *Journal of Physical Chemistry* **1976**, *80*(21), 2352–2362.
[50] I. C. Sanchez, R. H. Lacombe, Statistical thermodynamics of polymer solutions. *Macromolecules* **1978**, *11*(6), 1145–1156.
[51] C. H. Ortiz-Estrada, Comportamiento de soluciones poliméricas en CO_2 supercrítico. Simulación, experimentación y modelación. ScD. Thesis, 2003, México.
[52] G. Luna-Bárcenas, S. Mawson, S. Takishima, J. M. DeSimone, I. C. Sanchez, K. P. Johnston, Phase Behavior of Poly(1,1-Dihydroperfluorooctylacrylate) in Supercritical Carbon Dioxide. *Fluid Phase Equilibria* **1998**, *146*(1,2), 325–337.
[53] Y. Chernyak, F. Henon, R. B. Harris, R. D. Gould, R. K. Franklin, J. R. Edwards, J. M. DeSimone, R. G. Carbonell, Formation of Perfluoropolyether Coatings by the Rapid Expansion of Supercritical Solutions (RESS) Process. Part 1: Experimental Results. *Ind. Eng. Chem. Res.* **2001**, *40*(26), 6118–6126.
[54] A. Blasig, C. Shi, R. M. Enick, M. C. Thies, Effect of Concentration and Degree of Saturation on RESS of a CO_2-Soluble Fluoropolymer. *Ind. Eng. Chem. Res.* **2002**, *41*(20), 4976–4983.
[55] S. Mawson, K. P. Johnston, J. R. Combes, J. M. DeSimone, Formation of Poly(1,1,2,2-tetrahydroperfluorodecyl acrylate) Submicron Fibers and Particles from Supercritical Carbon Dioxide Solutions. *Macromolecules* **1995**, *28*(9), 3182–3191.
[56] Y. Xiong, E. Kiran, High-Pressure Phase Behavior in Polyethylene/n-Butane Binary and Polyethylene/n-Butane/CO_2 Ternary Systems. *Journal of Applied Polymer Science* **1994**, *53*(9), 1179–1190.

[57] E. Kiran, Y. Xiong, Miscibility of Isotactic Polypropylene in n-Pentane and n-Pentane + Carbon Dioxide Mixtures at High Pressures. *J. of Supercritical Fluids* **1998**, *11*(3), 173–177.
[58] I. Nagy, W. de Loos Th, R. A. Krenz, R. A. Heidemann, High Pressure Phase Equilibria in the Systems Linear Low Density Polyethylene + n-Hexane and Linear Low Density Polyethylene + n-Hexane + Ethylene: Experimental Results and Modelling with Sanchez-Lacombe Equation of State. *J. of Supercritical Fluids* **2006**, *37*(1), 115–124.
[59] I. Nagy, R. A. Krenz, R. A. Heidemann, W. de Loos Th, High-Pressure Phase Equilibria in the System Linear Low Density Polyethylene + Isohexane: Experimental Results and Modelling. *J. of Supercritical Fluids* **2007**, *40*(1), 125–133.
[60] S. M. Joung, J.-U. Park, S. Y. Kim, K.-P. Yoo, High-Pressure Phase Behavior of Polymer-Solvent Systems with Addition of Supercritical CO_2 at Temperatures from 323.15 K to 503.15 k. *J. Chem. Eng. Data* **2002**, *47*(2), 270–273.
[61] P. M. Ndiaye, C. Dariva, J. V. Oliveira, F. W. Tavares, Phase Behavior of Isotactic Polypropylene/C4-Solvents at High Pressure. Experimental Data and SAFT Modeling. *J. of Supercritical Fluids* **2001**, *21*(2), 93–103.
[62] T. M. Martin, A. A. Lateef, C. B. Roberts, Measurements and Modeling of Cloud Point Behavior for Polypropylene/n-Pentane and Polypropylene/n-Pentane/Carbon Dioxide Mixtures at High Pressure. *Fluid Phase Equilibria* **1999**, *154*(2), 241–259.
[63] P. F. Arce, M. Aznar, Phase Behavior of Polypropylene + n-pentane and Polypropylene + n-Pentane + Carbon Dioxide: Modeling with Cubic and Non-Cubic Equation of State. *J. of Supercritical Fluids* **2005**, *34*(2), 177–182.
[64] L. Zeman, J. Biros, G. Delmas, D. Patterson, Pressure Effects in Polymer Solution Phase Equilibria. I. The Lower Critical Solution Temperature of Polyisobutylene and Polydimethylsiloxane in Lower Alkanes. *The Journal of Physical Chemistry* **1972**, *76*(8), 1206–1213.
[65] N. Koak, R. M. Visser, W. de Loos, Th, High-Pressure Phase Behavior of the Systems Polyethylene + Ethylene and Polybutene + 1-Butene. *Fluid Phase Equilibria* **1999**, *158–160*, 835–846.
[66] H.-S. Byun, K.-P. Yoo, Phase Behavior of the Poly[Octyl (Meth)acrylate] + Supercritical Fluid Solvents + Monomer and CO_2 + Monomer Mixtures at High Pressure. *J. of Supercritical Fluids* **2007**, *41*(3), 472–481.
[67] H.-S. Byun, D.-H. Lee, Phase Behavior of Binary and Ternary Mixtures of Poly(Decylacrylate)-Supercritical Solvents-Decyl Acrylate and Poly(decylmethacrylate)-CO_2-Decyl Methacrylate Systems. *Ind. Eng. Chem. Res.* **2006**, *45*(10), 3373–3380.
[68] H.-S. Byun, D.-H. Lee, Phase Behavior of the Poly(neopentyl methacrylate) + Supercritical Fluid Solvents + Neopenthyl Methacrylate System and CO_2 + Neopentyl Methacrylate Mixtures at High Pressure. *Polymer* **2007**, *48*(3), 805–812.
[69] Shuang. Liu, Dong.-Hyun. Lee, Hun.-Soo. Byun, Phase Behavior for Mixtures of Poly(2-ethylhexyl acrylate) + 2-Ethylhexyl Acrylate and Poly(2-ethylhexyl methacrylate) + 2-Ethylhexyl Methacrylate with Supercritical Fluid Solvents. *Journal of Chemical & Engineering Data* **2007**, *52*(2), 410–418.
[70] H.-S. Byun, M. A. McHugh, High Pressure Phase Behavior of Poly[Isopropyl Acrylate] and [Isopropyl Methacrylate] in Supercritical Fluid (SCF) Solvent and SCF Solvent + Cosolvent Mixtures. *J. of Supercritical Fluids* **2007**, *41*(3), 482–491.
[71] B. Bungert, G. Sadowski, W. Arlt, Supercritical Antisolvent Fraction: Measurements in the Systems Monodisperse and Bidisperse Polystyrene-Cyclohexane-Carbon Dioxide. *Fluid Phase Equilibria* **1997**, *139*(1–2), 349–359.
[72] L. Zeman, D. Patterson, Pressure Effects in Polymer Solution Phase Equilibria. II. Systems Showing Upper and Lower Critical Solution Temperatures. *The Journal of Physical Chemistry* **1972**, *76*(8), 1214–1218.
[73] C. W. Haschets, A. D. Shine, Phase Behavior of Polymer-Supercritical Chlorodifluoromethane Solutions. *Macromolecules* **1993**, *26*(19), 5052–5060.
[74] M. Lora, J. S. Lim, M. A. McHugh, Comparison of the Solubility of PVF and PVDF in Supercritical CH_2F_2 and CO_2 and in CO_2 with Acetona, Dimethyl Ether, and Ethanol. *J. Phys. Chem. B* **1999**, *103*(14), 2818–2822.
[75] Y.-M. Kuk, B.-C. Lee, Y. W. Lee, J. S. Lim, Phase Behavior of Biodegradable Polymers in Dimethyl Ether and Dimethyl Ether + Carbon Dioxide. *J. Chem. Eng. Data* **2001**, *46*(5), 1344–1348.
[76] Y.-M. Kuk, B.-C. Lee, Y. W. Lee, J. S. Lim, High-Pressure Phase Behavior of Poly(D,L-lactide) in Chlorodifluoromethane, Difluoromethane, Trifluoromethane, and 1,1,1,2-Tetrafluoroethane. *J. Chem. Eng. Data* **2002**, *47*(3), 575–581.
[77] J. S. Lim, J.-Y. Park, C. H. Yoon, Y.-W. Lee, K.-P. Yoo, Cloud Points of Poly(L-lactide) in HCFC-22, HFC-23, HFC-32, HFC-125, HFC-143a, HFC-152a, HFC-227ea, Dimethyl Ether (DME), and HCFC-22 + CO_2 in the Supercritical States. *J. Chem. Eng. Data* **2004**, *49*(6), 1622–1627.
[78] J. M. Lee, B.-C. Lee, S.-H. Lee, Cloud Points of Biodegradable Polymers in Compressed Liquid and Supercritical Chlorodifluoromethane. *J. Chem. Eng. Data* **2000**, *45*(5), 851–856.
[79] B.-C. Lee, J. S. Lim, Y.-W. Lee, Effect of Solvent Composition and Polymer Molecular Weight on Cloud Points of Poly(L-lactide) in Chlorodifluoromethane + Carbon Dioxide. *J. Chem. Eng. Data* **2003**, *48*(4), 774–777.
[80] H.-S. Byun, D.-H. Lee, J.-S. Lim, K.-P. Yoo, Phase Behavior of the Binary and Ternary Mixtures

of Biodegradable Poly(ε-caprolactone) in Supercritical Fluids. *Ind. Eng. Chem. Res.* **2006**, *45*(10), 3366–3372.
[81] R. F. Blanks, J. M. Prausnitz, Thermodynamics of Polymer Solubility in Polar and Nonpolar Systems. *Ind. Eng. Chem. Fundamentals* **1964**, *3*(1), 1–8.
[82] D. L. Ho, C. J. Glinka, New insights into Hansen's solubility parameters. *Journal of Polymer Science, Part B: Polymer Physics* **2004**, *42*(23), 4337–4343.
[83] M. J. El-Hibri, W. Cheng, P. Munk, Inverse Gas Chromatography. 6. Thermodynamics of Poly(ε-caprolactone)-Polyepichlorohydrin Blends. *Macromolecules* **1988**, *21*(12), 3458–3463.
[84] J.-C. Huang, R. D. Deanin, Multicomponent solubility parameters of poly(vinyl chloride) and poly(tetramethylene glycol). *Fluid Phase Equilibria* **2005**, *227*(1), 125–133.
[85] V. Kanellopoulus, D. Mouratides, P. Pladis, C. Kiparissides, Prediction of Solubility of α-Olefins in Polyolefins Using a Combined Equations of State-Molecular Dynamics Approach. *Ind. Eng. Chem. Res.* **2006**, *45*(17), 5870–5878.
[86] I. C. Sanchez, C. Panayiotou, Equation of State Thermodynamics of Polymer and Related Solutions., In: *Models for Thermodynamics and Phase Equilibria Calculations*, S. Sandler, Ed., Marcel Dekker Inc., New York **1994**.
[87] P. Arce, M. Aznar, Modeling the Phase Behavior of Commercial Biodegradable Polymers and Copolymer in Supercritical Fluids. *Fluid Phase Equilibria* **2005**, *238*(2), 242–253.
[88] P. Arce, M. Aznar, Modeling the Thermodynamic Behavior of Poly(lactide-co-glycolide) + Supercritical Fluid Mixtures with Equations of State. *Fluid Phase Equilibria* **2006**, *244*(1), 16–25.
[89] E. C. Ihmels, E. W. Lemmon, Experimental densities, vapor pressures, and critical point, and a fundamental equation of state for dimethyl ether. *Fluid Phase Equilibria* **2006**, in press.
[90] A. E. Bozdogan, A method for determination of thermodynamic and solubility parameters of polymers from temperature and molecular weight dependence of intrinsic viscosity. *Polymer* **2004**, *45*(18), 6415–6424.
[91] A. E. Bozdogan, A method for determination of thermodynamics and solubility parameters of polymers in dilute solutions from critical volume fractions. *Polymer* **2003**, *44*(20), 6427–6430.
[92] T. Lindvig, M. L. Michelsen, G. M. Kontogeorgis, A Flory-Huggins model based on the Hansen solubility parameters. *Fluid Phase Equilibria* **2002**, *203*(1–2), 247–260.
[93] A. Agrawal, A. D. Saran, S. S. Rath, A. Khanna, Constrained nonlinear optimization for solubility parameters of poly(lactic acid) and poly(glycolic acid)-validation and comparison. *Polymer* **2004**, *45*(25), 8603–8612.
[94] U. Siemann, The solubility parameter of poly(D,L-lactic acid). *European Polymer Journal* **1992**, *28*(3), 293–297.
[95] S. Schenderlein, M. Lueck, B. W. Mueller, Partial solubility parameters of poly(D,L-lactide-co-glycolide). *International Journal of Pharmaceutics* **2004**, *286*(1–2), 19–26.
[96] P. Zoller, D. J. Walsh, *Standard Pressure-Volume-Temperature Data for Polymers*, Technomic Publishing Co., Inc., Lancaster, PA 1995.
[97] B. J. Briscoe, O. Lorge, A. Wajs, P. Dang, Carbon Dioxide-Poly(Vinylidene Fluoride) Interactions at High Pressure. *Journal of Polymer Science: Part B: Polymer Physics* **1998**, *36*(13), 2435–2447.
[98] C. W. Haschets, A. D. Shine, Phase Behavior of Polymer-Supercritical Chlorodifluoromethane Solutions. *Macromolecules* **1993**, *26*(19), 5052–5060.
[99] X. Kong, M. D. L. V. Silveira, L. Zhao, P. Choi, A Pseudo Equation-of-State Approach for the Estimation of Solubility Parameters of Polyethylene by Inverse Gas Chromatography. *Macromolecules* **2002**, *35*(22), 8586–8590.
[100] J.-C. Huang, Methods to determine solubility parameters of polymers at high temperature using inverse gas chromatography. *Journal of Applied Polymer Science* **2004**, *94*(4), 1547–1555.
[101] J.-C. Huang, Methods to determine solubility parameters of polymers using inverse gas chromatography. *Journal of Applied Polymer Science* **2004**, *91*(5), 2894–2902.
[102] K. Adamska, A. Voelkel, Hansen solubility parameters for polyethylene glycols by inverse gas chromatography. *Journal of Chromatography, A* **2006**, *1132*(1–2), 260–267.
[103] P. Bustamante, J. Navarro-Lupion, B. Escalera, A new method to determine the partial solubility parameters of polymers from intrinsic viscosity. *European Journal of Pharmaceutical Sciences* **2005**, *24*(2–3), 229–237.
[104] R. K. Franklin, J. R. Edwards, Y. Chernyak, R. D. Gould, F. Henon, R. G. Carbonell, Formation of Perfluoropolyether Coatings by the Rapid Expansion of Supercritical Solutions (RESS) Process. Part 2: Numerical Modelling. *Ind. Eng. Chem. Res.* **2001**, *40*(26), 6127–6139.

